ANALYSIS AND DESIGN OF A POINT-SOURCE INTEGRATING-CAVITY ABSORPTION METER

Robert A. Leathers, T. Valerie Downes, Curtiss O. Davis, and Gia M. Lamela
Naval Research Laboratory, Code 7212, 4555 Overlook Ave., SW,
Washington, DC 20375

ABSTRACT

A prototype point-source integrating-cavity absorption meter (PSICAM) is being constructed at NRL for the investigation of coastal ocean waters. We evaluated the theoretical performance of the PSICAM with Monte Carlo simulations and a sensitivity analysis. The scattering errors were found to be negligible for visible wavelengths. The precision of the absorption measurements depends greatly on the values and uncertainties of the reference solutions.

INTRODUCTION

The measurement of the absorption coefficient of sea water and its components is of great importance for oceanography and optical remote sensing of the ocean. There are several methods for determining its value, including the quantitative filter technique (Roesler, 1998), the ac-9 (Moore, 1994), and the use of underwater measurements of the natural light (Gordon, 1998; Leathers, 1999). Each of these methods has errors associated with the difficulty of separating absorption effects from scattering effects. An alternative to these approaches is the use of an integrating-cavity absorption meter (ICAM), which is designed to provide a measurement that is insensitive to scattering.

The use of an ICAM was suggested by Elterman (1970) for solids and was adapted to sea water by Fry, Kattawar, and Pope (1992). The sea-water configuration consists of a cavity completely filled with the water sample and a second integrating cavity surrounding the first. The cavity walls are made of a highly reflective material. An isotropic light field is generated between the two cavities that diffuses into the inner cavity, providing to the inner cavity a diffuse light source that is uniform over the cavity walls. Kirk (1995) proposed that the two cavities be made spherical and concentric, making it possible to analytically model the relationship between the absorption coefficient and the ICAM detector response.

Later Kirk (1997) proposed a different ICAM design in which the spherical cavity containing the water sample is illuminated with an isotropic source at the center of the sphere. The primary advantage of this point-source integrating-cavity absorption meter (PSICAM) is that an outer cavity is unnecessary. Kirk (1997) provides analytical equations for obtaining the absorption coefficient with a PSICAM and includes some error analysis.

In this work we extend Kirk's PSICAM analysis in preparation for the construction of a prototype instrument that will be used at the Naval Research Laboratory for the investigation of coastal ocean waters. Here we describe the prototype, review Kirk's equations for the PSICAM operation, quantify the scattering errors in these equations, and predict the PSICAM performance with a sensitivity analysis.

PROTOTYPE DESIGN

The prototype design follows the spirit of that proposed by Kirk (1997); however, the components and materials are completely different. The PSICAM body was manufactured by Labsphere (North Sutton, NH) of Spectralon, a Labsphere proprietary material with a reflectance of 0.99. However, it is the space where there is nothing that the usefulness of the vessel depends (Lao Tsu, 500 B.C.). The cavity radius is 5 cm and has four ports: fill, drain, source, and detector. The diffuse source is generated by passing a fiber optic source into a 3/4-inch-diameter solid Teflon sphere, the same sphere used by Biospherical Instruments Inc. (San Diego, CA) for its PAR sensors. The detector is a fiber-optic radiance detector with a Gershun tube extension to narrow its field of view.

BASIC EQUATIONS

The outwardly directed irradiance F_0 at the inner wall of a perfectly symmetrical PSICAM is proportional to the average number of times a photon collides with the wall, N_C, before being absorbed either by the fluid in the cavity or by the cavity wall (Kirk, 1995; Kirk, 1997). The transmittance T_{AB}, which is the ratio of the measured values of F_0 when the cavity is filled with samples A and B, respectively, is therefore

$$T_{AB} = \frac{F_0^A}{F_0^B} = \frac{N_C^A}{N_C^B}. \tag{1}$$

The value of N_C equals the number of photons reaching the wall from the source for the first time plus the number of photons colliding with the wall a second time, etc.,

$$N_C = P_0 + P_0 \rho^2 P_S^2 + \ldots = P_0 \sum_{n=0}^{\infty} \left(\rho \ P_S\right)^n = P_0 / \left(1 - \rho \ P_S\right), \tag{2}$$

where P_0 is the probability that a photon leaving the source at the center reaches the wall (i.e., without being absorbed by the fluid), P_s is the probability that a photon leaving the wall will return to the wall, and ρ is the wall reflectivity. Combining Eqs. (1) and (2),

$$T_{AB} = \frac{P_0^A \left(1 - \rho \ P_S^B\right)}{P_0^B \left(1 - \rho \ P_S^A\right)}. \tag{3}$$

For a central point-source, the value of P_0 for a non-scattering solution is

$$P_0(a, r) = \exp(-ar), \tag{4}$$

where a is the absorption coefficient of the sample and r is the inner radius of the PSICAM cavity. Similarly, for diffuse light leaving the spherical cavity wall the value of P_s for a non-scattering fluid is (Kirk, 1995)

$$P_S(a, r) = \frac{1}{2a^2 r^2}\left[1 - \exp(-2ar)(2ar + 1)\right]. \tag{5}$$

From Eqs. (3)—(5), the transmittance of a non-scattering fluid in a PSICAM with a diffuse cavity wall is

$$T_{AB} = \frac{\exp(-a_A r)\left[1 - \rho \ P_S(a_B, r)\right]}{\exp(-a_B r)\left[1 - \rho \ P_S(a_A, r)\right]}, \tag{6}$$

with $P_s(a,r)$ given by Eq. (5). Kirk (1997) indicates that both P_0 and P_s are insensitive to the presence of scattering for most practical ocean optics purposes and that Eq. (6) can

therefore be applied to seawater samples even though scattering was ignored in their derivation.

Equation (6) can be used in two ways. First, when the absorption coefficients of samples *A* and *B* are known the wall reflectivity can be determined from the measurement of T_{AB} with the solution of Eq. (6) (Kirk, 1997),

$$\rho = \frac{T_{AB}\exp(-a_B r) - \exp(-a_A r)}{T_{AB}\exp(-a_B r)P_S(a_A, r) - \exp(-a_A r)P_S(a_B, r)}. \quad (7)$$

Second, from Eq. (6) we can express the transmittance *T* of a fluid of interest with unknown absorption coefficient *a* with respect to a reference sample R with known absorption coefficient a_{ref},

$$T = \exp\left[-r(a - a_{ref})\right]\left(\frac{1-\rho\ P_S(a_{ref}, r)}{1-\rho\ P_S(a, r)}\right). \quad (8)$$

The value of *a* can therefore be determined from the measurement of *T* with an iterative solution of Eq. (8).

If a radiance detector is used rather than an irradiance detector, the sensor should be arranged so that the source is not in the sensor's field of view. Also, Eq. (2) would be replaced with the approximation

$$N_C = \rho\, P_0\, P_s / (1-\rho\, P_s), \quad (9)$$

and Eqs. (6)—(8) must be modified accordingly.

SCATTERING EFFECTS

Equations (4) and (5) for the probabilities of photon survival P_0 and P_s were derived for non-scattering absorbers. We quantified the effects of scattering on the values of P_0, P_s, and N_C with Monte Carlo simulations. The values of P_0 and P_s were computed separately, and Eq. (2) was used to determine N_C for specific values of ρ. Each photon path was determined by random numbers *R* evenly distributed on the range [0,1]. Specifically, each photon pathlength *s* was found from

$$s = -(1/c)\ln(1-R), \quad (10)$$

where *c* is the attenuation coefficient (m^{-1}). At each scattering event, the azimuthal scattering angle with respect to the incident direction was found with

$$\Phi = 2\pi R. \quad (11)$$

The cosine of the polar scattering angle with respect to the incident direction μ_s was found either by taking $\mu_s = 1-2R$ for isotropic scattering or by solving for μ_s in

$$C(\mu_s) = R, \quad (12)$$

where the cumulative distribution function $C(\mu_s)$ was taken to be the average of those provided by Petzold (1972) for the three samples from San Diego Harbor. For each scattering event, the new direction cosines of the photon (α', β', γ') were computed from the initial photon direction cosines (α, β, γ) and scattering angles (polar angle Θ, azimuthal angle Φ) with

$$\begin{bmatrix}\alpha'\\ \beta'\\ \gamma'\end{bmatrix}=\begin{bmatrix}\alpha\gamma/q & -\beta/q & \alpha\\ \beta\gamma/q & \alpha/q & \beta\\ -q & 0 & \gamma\end{bmatrix}\begin{bmatrix}\alpha_s\\ \beta_s\\ \gamma_s\end{bmatrix},\ (\gamma^2<1), \tag{13a}$$

$$\begin{bmatrix}\alpha'\\ \beta'\\ \gamma'\end{bmatrix}=sign(\gamma)\begin{bmatrix}\alpha_s\\ \beta_s\\ \gamma_s\end{bmatrix},\ (\gamma^2=1) \tag{13b}$$

where $q=\sqrt{1-\gamma^2}$, $\alpha_s = \sin\Theta\cos\Phi$, $\beta_s = \sin\Theta\sin\Phi$, and $\gamma_s = \cos\Theta$.

The presence of scattering decreases the value of P_0 over its non-scattering value by increasing the effective path length of each photon from the source to the wall. Therefore Eq. (4) overestimates the true value of P_0. The percentage error in Eq. (4) was found to increase roughly linearly with respect to b and to be greatest for large values of a and r. The error for Petzold scattering was much smaller than that for isotropic scattering because for Petzold scattering the photons are scattered predominantly in the near-forward direction. For example, the percentage error in P_0 determined from Eq. (4) is shown versus b in Fig. 1 for radius r=0.05 m, wall reflectivity ρ=0.99, and absorption coefficient a= 1 m^{-1}. For isotropic scattering the error in Eq. (4) is approximately 0.9% and 11% for b=10 m^{-1} and b=100 m^{-1}, respectively, whereas for Petzold scattering the error in Eq. (4) is only about 0.6% and 0.04%, respectively. For a=0.1 m^{-1}, the errors were only about 1/10th of those for a=1 m^{-1}.

When a photon traveling from the wall back to the wall is scattered, its effective path length may be smaller or larger than it would have been if unscattered, depending on where, and into which direction, it is scattered. For small values of a, b, and r it was found that the overall (statistical) scattering effect is negligible. For large values of a, b, or r, however, it is more likely that a photon will be scattered back to the wall near where it left, thus increasing the value of P_s. Equation (5) therefore underestimates the true value of P_s for large values of a, b, and r. Although the scattering error in P_s is generally very small, the total PSICAM response is proportional to $1/(1-\rho P_s)$, which for large values of ρ is very sensitive to the value of P_s. The percentage error in $1/(1-\rho P_s)$ is shown in Fig. 1 for r=0.05 m, ρ=0.99, and a=1 m^{-1}. Its magnitude increases approximately linearly with increasing values of b but is about 1/3 that of the error in P_0.

Because scattering affects P_0 and P_s in opposite ways, the percentage error in F_0 (which equals the percentage error in N_C) is smaller than that in either P_0 or P_s. The error in the PSICAM response predicted by Eqs. (4) and (5) is shown in Fig. 2 for Petzold scattering. The scattering effect on F_0 was found to be insignificant for most oceanic problems; even for the extremely large value of b=100 the error in F_0 for Petzold scattering is less than 0.35% when a<1 m^{-1}. However, the scattering effects may be important in the infrared wavelengths (for which a>1 m^{-1}).

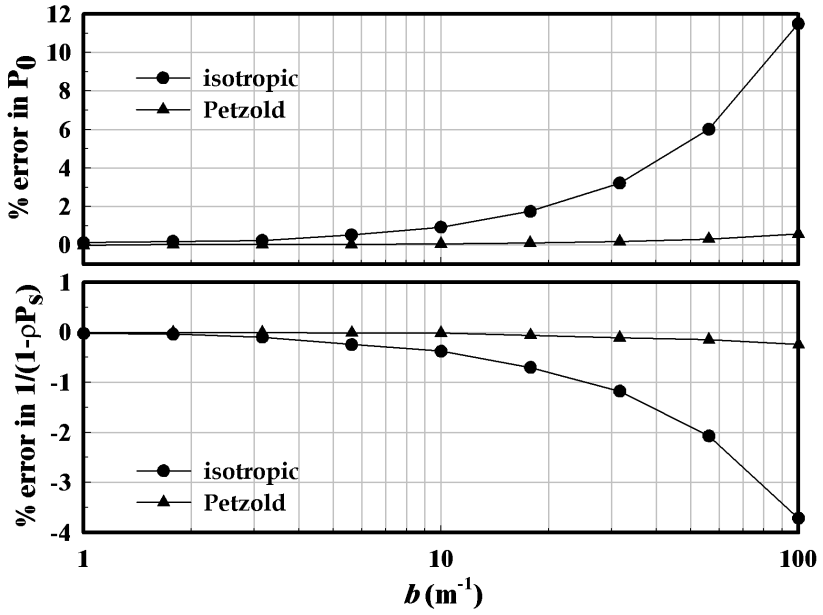

Figure 1. Percentage scattering errors in Eqs. (4) and (5) for the probabilities of source-to-wall photon survival (P_0) and wall-to-wall photon survival (P_s) for isotropic and Petzold scattering (a=0.3 m^{-1}, r=0.05 m).

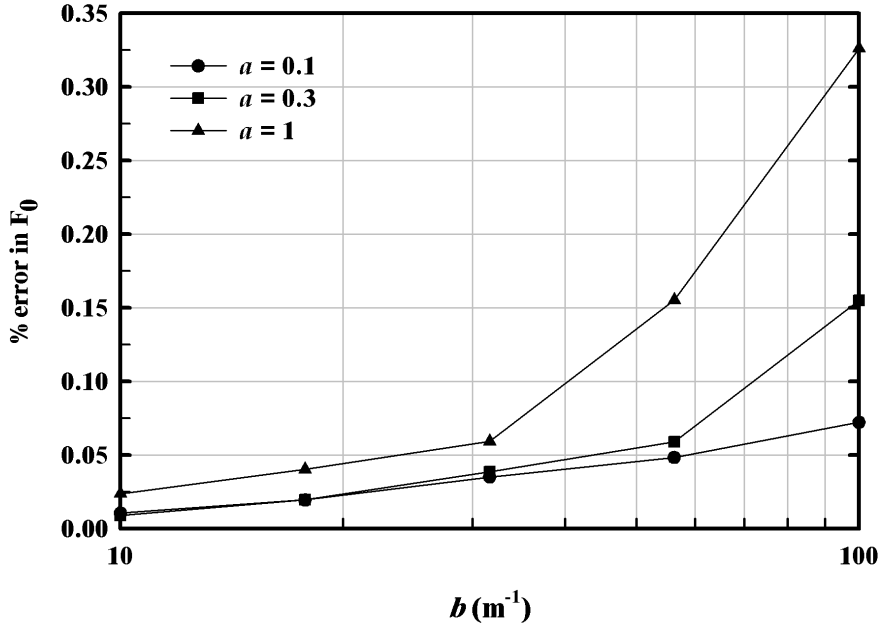

Figure 2. Percentage error in the PSICAM response predicted by Eqs. (2), (4), and (5) due to the presence of sea-water scattering for r=0.05 m, ρ=0.99, and a=0.1, 0.3, and 1.0 m^{-1}.

SENSITIVITY ANALYSIS

We performed a sensitivity analysis on Eqs. (6)—(8) to determine the uncertainty in the value of a given the uncertainties in the PSICAM measurements and properties. For the mode of operation in which the cavity-wall reflectivity ρ is assumed to be known from direct measurement, the precision in a_{ref} and ρ were found to be important, whereas the uncertainties in r and T were typically insignificant. Estimates of a are particularly sensitive to ρ, with the uncertainty in a being one to two orders of magnitude larger than that in ρ. Therefore the value of ρ must be known very precisely to use the PSICAM in this way.

For the mode of operation in which ρ is instead determined from PSICAM measurements of two non-scattering samples of known absorption coefficient values [i.e., with Eq. (7)], the precision of a depends primarily on the uncertainties of the two reference solutions. The high sensitivity of a to ρ is compensated for by the very low sensitivities of ρ to a_{A} and a_{B}. The best results are obtained when $a_A \approx a$.

CONCLUSIONS

We found the scattering errors in Eqs. (4) and (5) to be insignificant for most ocean optics problems. However, they may be important for near-IR wavelengths where the value of a is large.

If the value of the PSICAM wall reflectivity is known, the absorption coefficient of a sample can be determined [with Eq. (8)] from PSICAM measurements of the sample and of a reference solution. Because of the high sensitivity of a to ρ, however, the uncertainty in the result may be unacceptably large unless ρ is known to high precision.

Alternatively, a generally more precise estimate of a can be obtained by including the PSICAM measurement of a least one additional reference solution, eliminating the need to know the value of the wall reflectivity *a priori*. Even if the value of ρ is known from direct measurement, it may be preferable to determine it with Eq. (7) since this tends to eliminate errors associated with the measurements of ρ, r and a_{ref}.

A more detailed analysis of the PSICAM has been prepared for publication. A prototype PSICAM is currently under construction, and we intend to also publish a description of the instrument design and laboratory experiments once they have been completed. Other issues being addressed include the effects of anisotropy in the light source, the size of the light source, and the ports in the cavity wall.

ACKNOWLEDGMENTS

We gratefully acknowledge the support of the U. S. Office of Naval Research. This work was inspired by a presentation by John Kirk at the European Joint Research Center in Ispra, Italy in July 1999.

REFERENCES

P. Elterman (1970), Integrating cavity spectroscopy, *Appl. Opt.* **9**, 2140--2142.

E. S. Fry, G. Kattawar, and R. M. Pope (1992), Integrating cavity absorption meter, *Appl. Opt.* **31**, 2055--2065.

H. R. Gordon and G. C. Boynton (1998), Radiance--irradiance inversion algorithm for estimating the absorption and backscattering coefficients of natural waters: vertically stratified water bodies, *Appl. Opt.* **37**, 3886--3896.

J. T. O. Kirk (1995), Modeling the performance of an integrating-cavity absorption meter: theory and calculations for a spherical cavity, *Appl. Opt.* **34**, 4397--4408.

J. T. O. Kirk (1997), Point-source integrating-cavity absorption meter: theoretical principles and numerical modeling, *Appl. Opt.* **36**, 6123--6128.

Lao Tsu (circa 500 B.C.), Tao Te Ching.

R. A. Leathers, C. S. Roesler, and N. J. McCormick (1999), Ocean inherent optical property determination from in-water light measurements, *Appl. Opt.* **38**, 5096--5103.

C. Moore (1994), In situ biochemical, oceanic, optical meters, *Sea Technology* **35**, 10--16.

T. J. Petzold (1972), Volume scattering functions for selected ocean waters, SIO Ref. 72-78 (Scripps Institution of Oceanography, La Jolla, Calif.).

C. S. Roesler (1998), Theoretical and experimental approaches to improve the accuracy of particulate absorption coefficients derived from the quantitative filter technique, *Limnol. Oceanogr.* **43** , 1649--1660.